Orbital-ordering driven structural distortion in metallic $SrCrO_3$

K.-W. Lee[1,2] and W. E. Pickett[1]
[1]*Department of Physics, University of California, Davis, California 95616, USA*
[2]*Department of Display and Semiconductor Physics, Korea University, Jochiwon, Chungnam 339-700, Korea*
(Received 4 May 2009; revised manuscript received 14 July 2009; published 30 September 2009)

In contrast to the previous reports that the divalent perovskite $SrCrO_3$ was believed to be cubic structure and nonmagnetic metal, recent measurements suggest coexistence of majority tetragonally distorted weak antiferromagnetic phase and minority nonmagnetic cubic phase. Within the local (spin) density approximation [L(S)DA] our calculations confirm that a slightly tetragonally distorted phase indeed is energetically favored. Using the correlated band theory method (LDA+Hubbard U) as seems to be justified by the unusual behavior observed in $SrCrO_3$, above the critical value $U_c=4$ eV only the distorted phase undergoes an orbital-ordering transition, resulting in $t_{2g}^2 \rightarrow d_{xy}^1(d_{xz}d_{yz})^1$ corresponding to the filling of the d_{xy} orbital but leaving the other two degenerate. The Fermi surfaces of the cubic phase are simple with nesting features, although the nesting wave vectors do not correlate with known data. This is not uncommon in perovskites; the strongly directional $d-d$ bonding often leads to boxlike Fermi surfaces and either the nesting is not strong enough or the matrix elements are not large enough to promote instabilities. Fixed spin moment calculations indicate the cubic structure is just beyond a ferromagnetic Stoner instability [$IN(0) \approx 1.1$] in L(S)DA and that the energy is unusually weakly dependent on the moment out to $1.5\mu_B$/Cr (varying only by 11 meV/Cr), reflecting low-energy long-wavelength magnetic fluctuations. We observe that this system shows strong magnetophonon coupling (change in Cr local moment is $\sim 7.3\mu_B/\text{Å}$) for breathing phonon modes.

DOI: 10.1103/PhysRevB.80.125133 PACS number(s): 71.20.Be, 71.30.+h, 75.50.Ee

I. INTRODUCTION

Forty years ago, a few divalent chromate perovskites $\mathcal{A}CrO_3$ ($\mathcal{A}$=Pb,Sr,Ca), formally possessing the Cr^{4+} ion, were synthesized at high temperature ~1300 K and under high pressure 6–10 GPa by a few groups.[1–5] In spite of their atypical and controversial properties these systems have been little studied probably due to difficulty of synthesis. More recently a few groups have begun to revisit the $CaCrO_3$ and $SrCrO_3$ compounds.[6–9] Whether these systems are metallic, strongly correlated, and spin ordered is still controversial.[6–10]

Roth and DeVries reported an ordered moment of $1.9\mu_B$ and Curie-Weiss moment of $2.83\mu_B$ in the isovalent compound $PbCrO_3$ consistent with $S=1$ $Cr^{4+}(d^2)$.[1] Chamberland and Moeller synthesized a single crystal, which was semiconducting with 0.27 eV activation energy.[2] There was an anomaly at $T_1=240$ K, and an upturn at $T_2=160$ K, in susceptibility. The latter was thought to imply a G-type antiferromagnetic (AFM) ordering corresponding to antiparallel spin ordering between all nearest neighbor Cr^{4+} ions. Additionally, at $T_3=100$ K, the logarithmic resistivity shows a kink, implying another transition. The samples of both groups had a cubic structure with lattice constant $a \approx 4.00$ Å. Local (spin) density approximation [L(S)DA] calculations obtained a magnetic moment of $1.4\mu_B$, three quarters of the experimental value, but no band gap.[11] This difference points to interaction effects beyond those described by L(S)DA. Chamberland also synthesized a cubic $SrCrO_3$ with $a=3.818$ Å and concluded it to be a nonmagnetic (NM) metal.[3]

Goodenough *et al.* synthesized polycrystalline $CaCrO_3$, which is orthorhombic ($a=5.287$ Å, $b=5.316$ Å, and $c=7.486$ Å) and nonconducting (although probably due to polycrystallinity).[4] Weiher, Chamberland, and Gillson obtained a metallic single-crystal sample.[5] The susceptibility measurements showed two anomalies, a kink at 325 K and an upturn at 90 K. At the latter, which is recently identified as the Neel temperature T_N,[6,9] a kink in the resistivity data and decrease in volume by 2% from the powder diffraction studies were observed. The Curie-Weiss moment is high spin $3.7\mu_B$ recently confirmed by Zhou *et al.*[6] The reason of large difference from spin-only value of $2.8\mu_B$ for $S=1$ system is unresolved, however it was found that the susceptibility in $SrCrO_3$ did not follow a Curie-Weiss behavior so no local-moment value could be identified.

In more recent studies, Zhou *et al.* observed a smooth decrease in thermal conductivity of $CaCrO_3$ and $SrCrO_3$ compounds as temperature is lowered, in their interpretation characteristic of neither an insulator nor a metal.[6] They interpreted this unusual behavior as due to some unusual Cr–O bonding instability, supported by an increase in compressibility observed around 4 GPa. In contrast to Chamberland's initial suggestion,[3] Zhou *et al.* concluded that $SrCrO_3$ is NM and insulating. Komarek *et al.* reported antiferromagnetism with ordering wavevector $Q_M=(\frac{1}{2},\frac{1}{2},0)$ (in units of $\frac{2\pi}{a}$) and a saturation magnetic moment of $1.2\mu_B$, using superconducting quantum-interference-device susceptibility and neutron diffraction.[9] At T_N, in contrast to the preliminary observations,[5] no change in volume was apparent. They suggested $CaCrO_3$ is itinerant, but close to being localized, implying importance of correlation effects.[9,10] Additionally, no evidence of orbital ordering within the t_{2g} shell was observed.[9]

Attfield and co-workers have concentrated on $SrCrO_3$, using neutron-diffraction and synchrotron powder x-ray diffraction studies.[7,8] Below $T_N \approx 40$ K, most of their sample underwent a structure transition from a NM cubic phase to a AFM tetragonal phase but the two phases coexist even at low

T. In the tetragonal phase with only slightly inequivalent lattice parameters, at T_N there are no visible changes in volume or in averaged Cr-O distance, and additionally no kink in resistivity. The temperature dependent neutron-diffraction data imply orbital reoccupation $(d_{xy}d_{xz}d_{yz})^2 \rightarrow d^1_{xy}(d_{xz}d_{yz})^1$ in the tetragonal phase at or near T_N. Both phases are metallic, though showing high resistivity due to grain-boundary scattering.

In this paper, we will focus on $SrCrO_3$, which has been little studied theoretically to date. In Sec. III, in particular, we will address electronic structures of both NM cubic phase and AFM distorted phase and show that the inclusion of correlation effects leads to an orbital-ordering driven distortion while remaining metallic. In Sec. IV, we discuss the oxygen breathing vibration that shows quite strong magnetophonon coupling.

II. STRUCTURE AND CALCULATION

Attfield and co-workers suggested a small structure distortion involving relative displacement of Sr and O ions, leading to $\sqrt{2}a \times \sqrt{2}a \times 2a$ quadrupled supercell (space group: *Imma*, No. 74).[7] The corresponding AFM order we consider, which is $(\frac{1}{2},\frac{1}{2},\frac{1}{2})$ order in terms of the original perovskite cell, is a G-type AFM. Through more precise measurements, instead of the quadrupled supercell they more recently concluded a tetragonally distorted structure with $c/a \approx 0.992$ but negligible change in volume (less than 1%), which shows antiferromagnetic ordering at wavevector $Q_M = (\frac{1}{2},\frac{1}{2},0)$ (space group: $P4/mmm$, No. 123).[8] This AFM order is conventionally called C-type AFM. Although this tetragonal phase is dominant below T_N, a NM cubic phase also coexists, consistent with results of our calculations (see below).

We investigated both distorted structures as well as the cubic phase, using L(S)DA and the LDA+Hubbard U (LDA+U) method.[12,13] For the quadrupled supercell, only the planar O position is displaced along the ⟨001⟩ direction since negligible displacements in Sr and apical O were initially suggested.[7] We used the recent experimental lattice constant $a=3.811$ Å for the cubic structure and for the quadrupled supercell, and $a=3.822$ and $c=3.792$ Å for the tetragonal structure.[8] Our optimized lattice constants in the cubic phase within L(S)DA are 3.748 Å for NM and 3.76 Å for AFM, reflecting the usual small increase in volume associated with magnetism and the overbinding that is common in L(S)DA.

We have used the full-potential local-orbital code FPLO for our study. In FPLO-5,[14] basis orbitals were chosen as Cr($3s3p$)$4s4p3d$, Sr($4s4p$)$5s5p4d$, and O $2s2p3d$. (The orbitals in parentheses indicate semicore orbitals.) The Brillouin zone was sampled with a regular mesh containing 726 irreducible k points since a fine mesh is required for sampling the Fermi surface.

III. ELECTRONIC STRUCTURE

A. NM Cubic Phase within LDA

In Sec. III A we address the electronic structure of the NM cubic phase (observed above 40 K) using LDA. The band structure around the Fermi level E_F (the Cr d regime) is shown in Fig. 1 and the corresponding densities of states (DOSs) are displayed in Fig. 2. The one-third filled Cr t_{2g} manifold with width of 2 eV lies between −1.5 eV and 0.5 eV (we take E_F as the zero of energy). The unfilled Cr e_g manifold touches the t_{2g} manifold at the X point at 0.5 eV and extends to 4.5 eV, leading to the t_{2g}-e_g (midpoint) splitting of roughly 2.5 eV. Flat bands along the $\Gamma-X-M$ lines result in a sharp peak in the DOS at 0.5 eV, which otherwise does not have any distinguishing structures near E_F.

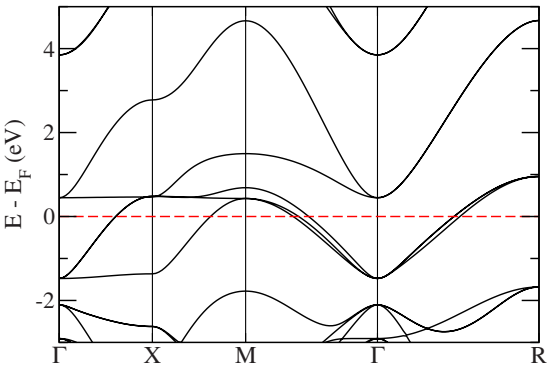

FIG. 1. (Color online) Enlarged band structure of NM $SrCrO_3$ in the region having mostly Cr d character. A flat band along the $\Gamma-X-M$ line lies at 0.5 eV. The O $2p$ states lie on the regime of −7.5 eV to −1.8 eV (not shown here). These symmetry points follow a simple-cubic notation (see Fig. 3). The R point is a zone boundary along ⟨111⟩ direction. The horizontal dashed line indicates the Fermi energy E_F.

The Fermi surfaces shown in Fig. 3 display nesting features, indicative of large susceptibilities at related wave vectors and suggesting the possibility of either magnetic or charge instabilities. The intersecting pipelike surface has six circular faces with a radius of $0.32(\frac{\pi}{a})$, so contains ~0.6 electrons per spin. Two cubelike surfaces with sides of length $\sim 0.61(\frac{2\pi}{a})$ are very similar in size and touch along the $\Gamma-X$ line.

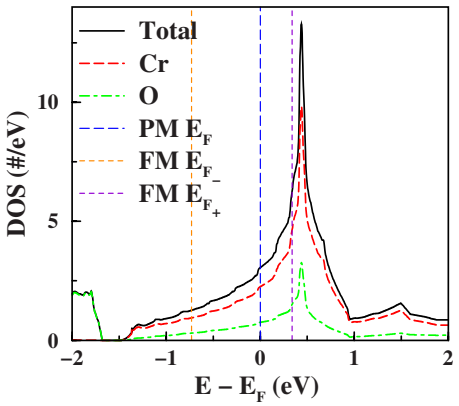

FIG. 2. (Color online) Total and atom-projected densities of states in NM $SrCrO_3$. A sharp peak lies at 0.5 eV while around E_F there is only a smoothly monotonic behavior. The DOS at E_F N(0) is 1.53 states per eV per spin, a quarter of which is contributed by O ions.

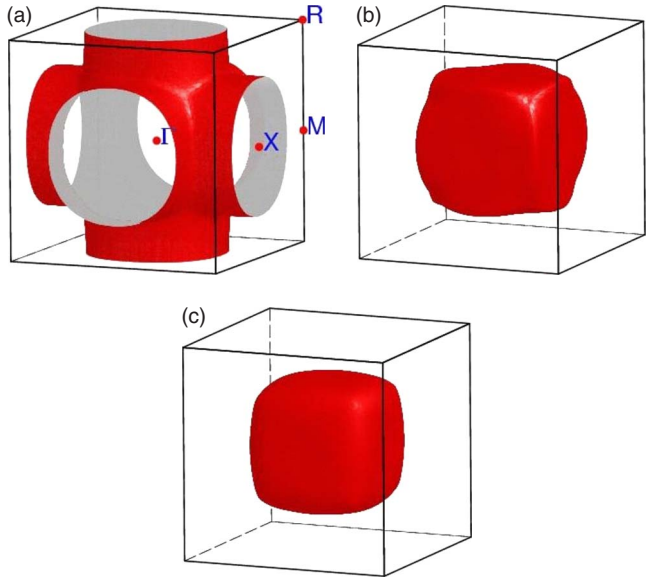

FIG. 3. (Color online) Fermi surfaces, which contain electrons of NM $SrCrO_3$. These surfaces show nesting features commonly arising in perovskite structure transition metal oxides. Both the second and the third surfaces are cubelike with rounded edges and corners; each face of the second surface is nearly circular. The Fermi velocity of 2×10^7 cm/sec, which is a typical value in a metal, is nearly uniform through the surfaces.

B. Structure Relaxation

Our L(S)DA calculations show this tetragonally distorted structure is energetically favored over the cubic structure. As expected from the small change in structure, however, the difference in energy is small, no more than 1 meV per Cr. The fact that these two structures are nearly degenerate is consistent with experimental observations. The quadrupled supercell, on the other hand, has a slightly higher energy than the cubic phase. In this section, we will focus on only the competing cubic and tetragonal phases.

To investigate sensitivity of this structure distortion to volume, we calculated the energy vs c/a relation in the range of $a=3.70-3.82$ Å. The volume is kept fixed while the c/a ratio of lattice parameters is varied since the experiment shows negligible change in volume between the two observed phases.[8] The result is given in Fig. 4. In very close agreement with experimental observations, a minimum occurs at $c/a=0.99$ for $a=3.82$ Å, which is the experimentally observed lattice parameter. However, with decreasing volume this distortion is gradually relieved and finally the cubic structure is favored energetically somewhat below $a\approx3.70$ Å, 0.06 Å smaller value than our optimized parameter.

C. Energetics

As discussed in the Introduction, the recent observations indicate the coexistence of NM cubic phase and AFM tetragonally distorted phase.[8] Within L(S)DA, AFM order is more favored energetically than NM in both crystal structures. In the tetragonal phase, AFM order ($M=1.55\mu_B$) is favored energetically over FM ($M=1.16\mu_B$) by 150 meV/Cr. The ferromagnetic state is favored only 11 meV/Cr over the nonmagnetic state. With Stoner $I=0.6$ eV (see below), the energy gain in a simple Stoner picture $IM^2/4$ would lead to much larger value of ~0.2 eV/Cr. Note that the moments are roughly consistent with $S=1$ ions in the presence of strong $p-d$ hybridization that is evident from the projected DOS in Fig. 2. The strong reduction in moments from the ionic value also reflects considerable hybridization so a fixed-local-moment (i.e., Heisenberg picture) has little use here. The behavior of ferromagnetic order will be investigated more explicitly below by fixed spin moment calculations.[15] The energy differences between magnetic phases are nearly independent of the small distortion that we study here.

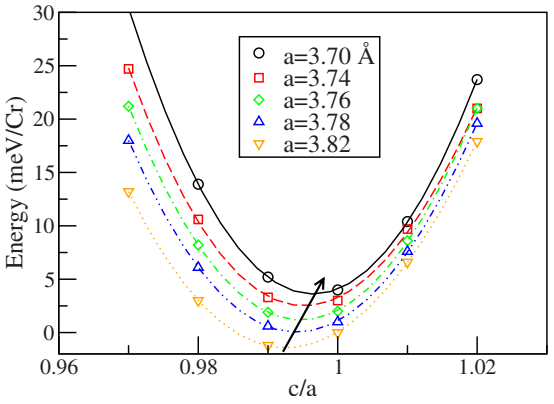

FIG. 4. (Color online) Changes in energy $SrCrO_3$ with respect to lattice-parameter ratio (c/a) in C-AFM phase with various choices of lattice parameter a. This a parameter in the range of 3.70–3.82 Å is approximately the range between our optimized value in the cubic structure and the experimentally observed value. The arrow denotes the change in position of the minima, pointing out the stronger structural distortion for larger volume.

D. Fixed Spin Moment (FSM) Studies

Initially we used a single Cr cell for our calculations, supplementing this with doubled cells (see below). Consistent with our L(S)DA calculations, the energy versus moment E(M) has a minimum at $M\sim1.3\mu_B$ and a related small gain of 11 meV in energy, as can be seen in curve in Fig. 5. The very flat E(M) behavior for M up to $1.5\mu_B$ indicates that magnetism in $SrCrO_3$ is very peculiar. The gain in exchange energy $IM^2/4$ is almost exactly compensated by a cost in other energy contributions across this range. The energy vs moment curve is fit at small M to the expression $\varepsilon-\varepsilon_0=\alpha M^2+\beta M^4$ to evaluate the Stoner (exchange) constant I from these FSM calculations.[15] The resulting value of $\alpha=-17$ meV/μ_B^2 (and $\beta=6$ meV/μ_B^4) provides the enhanced (observed) susceptibility given by

$$\chi=\frac{\chi_0}{1-N(0)I}\equiv\mathcal{S}\chi_0, \tag{1}$$

where the bare susceptibility is $\chi_0=2\mu_B^2N(0)$. The Stoner enhancement factor $\mathcal{S}=[2\alpha\chi_0]^{-1}$ is about −8. Thus the Stoner

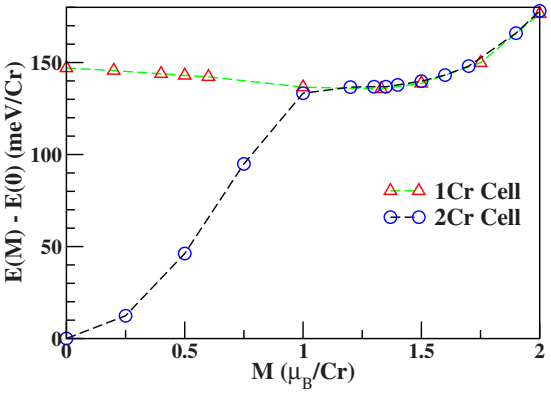

FIG. 5. (Color online) Fixed spin moment calculations using both one Cr and two Cr cells. The latter cell allows both NM and AFM states at moment $M=0$. For the doubled cell, the plot shows richer behavior (see text). Above $1\mu_B$ the states are the same simple FM aligned state.

$I=0.6$ eV, and $IN(0)=1.1$ with $N(0)=1.87$ states per eV per spin from our FM calculations, predicting the system is beyond the Stoner magnetic instability in the cubic phase [within L(S)DA].

To generalize the study, we used the two Cr supercell and started from C-AFM order (G-AFM order showed similar change) which also has total moment $M=0$. The magnetic field that is applied in the fixed spin moment method provides an evolution of the C-AFM state into a FM state, perhaps through an intermediate ferrimagnetic phase. A small systematic energy difference between the single and doubled cell energies that we compare has been accommodated by aligning the $M=0$ energies. We find the energy vs M curve to be comprised of three separate regimes: AFM at $M=0$ where the energy is ~ 150 meV/Cr lower than for NM; ferrimagnetic for $0<M\leq 1$ where the two Cr moments differ; then FM for $M>1$ where both calculations describe the same simple FM phase. While one might expect strong magnetoelastic coupling in this system, we find that our FSM results are insensitive to c/a ratio in the range given in Fig. 4.

E. L(S)DA Electronic Structure of the AFM Tetragonally Distorted Phase

Although Attfield and co-workers observed coexistence of the nonmagnetic cubic phase and the antiferromagnetic tetragonal phase, our L(S)DA calculations show energetically favored AFM in both phases, as already addressed. The C-AFM band structure is shown in Fig. 6. The Cr local moment is $1.55\mu_B$ with negligible dependence on this small tetragonal distortion. The largest effect of the structure distortion on the band structure occurs in the maxima at the M and R points, downshifting in energy at most 25 meV. The topmost band crossing E_F has the d_{xy} character.

IV. INCLUSION OF CORRELATION EFFECTS

L(S)DA predicts the C-AFM phase to be considerably lower in energy than the NM phase, in disagreement with experimental data that suggests the two phases are nearly

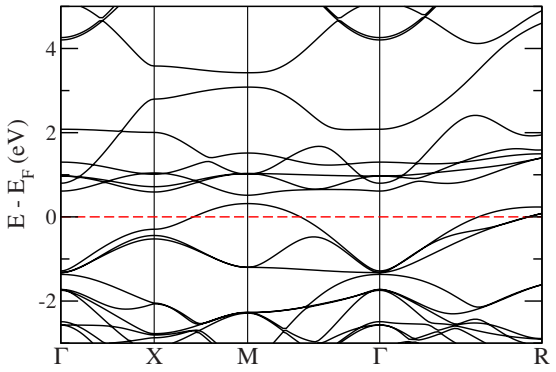

FIG. 6. (Color online) Enlarged band structure of C-AFM in the tetragonally distorted structure, plotted in the basal plane. That of the cubic phase with the same volume is similar, so is not shown. The antiferromagnetism introduces a gap at the X point in the range of $(-0.5)-(0.5)$ eV, and the t_{2g} bands become disconnected from the higher e_g bands due to the reduced bandwidths. In unit of π/a, the X point is (1/2,1/2,0).

degenerate. Also L(S)DA cannot produce the partially orbital order experimentally suggested. We address this discrepancy by including correlation within the LDA+U approach. Onsite Coulomb repulsion U was applied on the Cr ions with AFM order. U was varied in the range of 0–8 eV but the Hund's exchange integral $J=1$ eV is fixed since the results in the physical range of U are expected to be insensitive to J.

At $U=0=J$ (i.e., LSDA level), two electrons are evenly distributed in the three bands of the majority t_{2g} manifold. In the C-AFM (tetragonal) phase, increasing U changes occupancies with d_{xz} and d_{yz} weight transferring into d_{xy}. At $U_c=4$ eV, the majority d_{xy} band is fully occupied while the majority d_{xz} and d_{yz} bands share equally the other electron as shown in the orbital-projected DOS given in Fig. 7. This $d_{xy}^1(d_{xz}d_{yz})^1$ state is consistent with Attfield and co-workers' conclusion from their neutron-diffraction measurements.[8] This partial orbitally ordered arrangement remains for larger values of U. A potentially Mott-insulating $d_{xz}^1, d_{yz}^1, d_{xy}^0$ state is available but did not arise in the calculations. In the range of

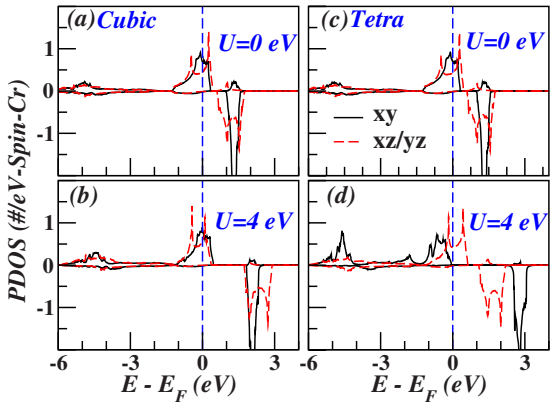

FIG. 7. (Color online) U-dependent orbital-projected densities of states of Cr t_{2g} states for (a)–(b) the cubic and (c)–(d) the tetragonal phase, at $U=0$ and 4 eV in C-AFM order. At $U=4$ eV, an orbit-ordering transition in d_{xy} orbital occurs in the tetragonal phase.

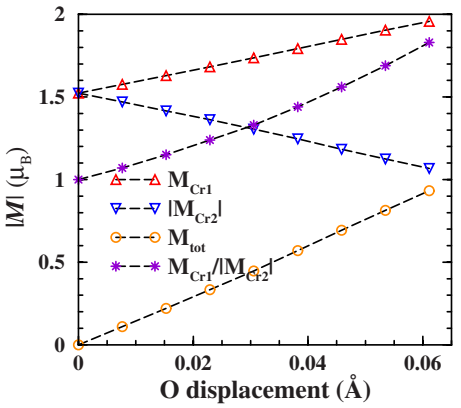

FIG. 8. (Color online) Change in moments due to the O breathing vibration when AFM allows. The Cr1, Cr2, and total moments are changed 7.1, −7.5, and $15.3\mu_B/\text{Å}$ in magnitude. Note that no displacement leads to AFM.

U studied here, this system remains metallic.

An orbital-ordering transition in a multiband system can result in significantly different bandwidths.[16] However, in this case, the difference in the occupied bandwidths is small, about 100 meV. The important change is that the center of the d_{xy} band lies roughly 1 eV lower than those of the partially occupied d_{xz}, d_{yz} bands. It is this difference in the band center (i.e., the on-site energy) that drives this transition, as happened in Na_xCoO_2 (Ref. 17) or V_2O_3.[18] Keeping the structure (and symmetry) cubic inhibits such an orbital-ordering transition, implying close interplay between structural distortion (even though tiny) and orbital ordering in LDA+U calculations in this system as suggested in $CaCrO_3$.[10]

V. O TILTING AND BREATHING PHONON MODES

To investigate another possibility of structure distortion in this perovskite, we used G-AFM order in the quadrupled supercell, which allows O tilting and breathing phonon modes in frozen phonon calculations within L(S)DA. However, our calculations show these distortions are unfavored energetically, resulting in stable phonon modes. These data of change in energy vs O displacement are fit well with a simple harmonic function. First, for the O tilting vibration the phonon energy is 38 meV, typical for metallic oxides. For the breathing mode the energy is 89 meV, corresponding to an rms displacement of the oxygen ions by 0.05 Å. (Allowing magnetic ordering, both frequencies reduce by ~5%.)

Our calculations show strong magnetophonon coupling for the breathing mode. When AFM ordering is included, the Cr local moment of $M_{\text{Cr}}=1.5\mu_B$ is modulated by about $\pm 7.3\mu_B/\text{Å}$, as shown in Fig. 8. These changes are quite large, even larger than the change in Fe moment, $6.8\mu_B/\text{Å}$, in LaFeAsO when As ions are displaced, which is widely discussed as unusually strong magnetophonon coupling.[19] At the rms displacement, the difference between Cr moments becomes $0.73\mu_B$, illustrating just how large the modulation in the moment by the breathing mode is. The Cr charge "disproportionation" due to O breathing also shows a value of $\pm 0.13e$ (i.e., a $0.26e$ charge difference) at the rms displacement, corresponding to a shift in charge of $\pm 2.6e/\text{Å}$.

VI. SUMMARY

We have presented and analyzed the electronic structure, magnetic ordering, and the impact of strong correlation effects in the perovskite material $SrCrO_3$, which is reported in a nonmagnetic cubic phase coexisting with an antiferromagnetic phase concurrent with a small distortion in structure below 40 K. Consistent with these observations, L(S)DA predicts the slightly distorted tetragonal structure, but overestimates the polarization energy. With L(S)DA the cubic phase is magnetically unstable with a Stoner product $IN(0)\approx 1.1$. The Fermi surface shows nesting features but they do not correlate with known data. Although it is possible for certain crystal symmetries for orbital ordering to occur without changing the crystal structure,[10] we have not pursued such possibilities.

Including correlated effects within the LDA+U approach, the distorted phase undergoes an orbital-ordering transition at a critical interaction strength $U_c=4$ eV, leading to $t_{2g}^2 \rightarrow d_{xy}^1(d_{xz}d_{yz})^1$ orbital ordering and structural transition to tetragonal structure. The structural symmetry lowering is crucial; the cubic phase remains a simple metal even for higher U. We have also demonstrated that the O breathing modes show strong magnetophonon coupling.

The magnetic behavior in $SrCrO_3$ remains unclear. The experimental data show weak magnetic behavior[8] and the susceptibility does not follow Curie-Weiss behavior.[6] In contrast to these observations, our various calculations always result in a full moment corresponding to $S=1$ configuration (reduced by hybridization) as expected for a d^2 ion. Without any peak in the DOS, the temperature variation cannot be modeled with temperature broadening as can be done, for example, in $TiBe_2$.[20]

ACKNOWLEDGMENTS

We acknowledge important communications with J. P. Attfield concerning his experimental observations, J.-S. Zhou for clarifying structure of $CaCrO_3$, and A. Kyker for illuminating discussion of temperature-dependent susceptibility. This work was supported by DOE under Grant No. DE-FG02-04ER4611, and interaction within DOE's Computational Materials Science Network is acknowledged. K.W.L. was partially supported by a Korea University under Grant No. K0718021.

[1] W. L. Roth and R. C. DeVries, J. Appl. Phys. **38**, 951 (1967); R. C. DeVries and W. L. Roth, J. Am. Ceram. Soc. **51**, 72 (1968).
[2] B. L. Chamberland and C. W. Moeller, J. Solid State Chem. **5**, 39 (1972).
[3] B. L. Chamberland, Solid State Commun. **5**, 663 (1967).
[4] J. B. Goodenough, J. M. Longo, and J. A. Kafalas, Mater. Res. Bull. **3**, 471 (1968).
[5] J. F. Weiher, B. L. Chamberland, and J. L. Gillson, J. Solid State Chem. **3**, 529 (1971).
[6] J.-S. Zhou, C.-Q. Jin, Y.-W. Long, L.-X. Yang, and J. B. Goodenough, Phys. Rev. Lett. **96**, 046408 (2006).
[7] A. J. Williams, A. Gillies, J. P. Attfield, G. Heymann, H. Huppertz, M. J. Martínez-Lope, and J. A. Alonso, Phys. Rev. B **73**, 104409 (2006).
[8] L. Ortega-San-Martin, A. J. Williams, J. Rodgers, J. P. Attfield, G. Heymann, and H. Huppertz, Phys. Rev. Lett. **99**, 255701 (2007).
[9] A. C. Komarek, S. V. Streltsov, M. Isobe, T. Moller, M. Hoelzel, A. Senyshyn, D. Trots, M. T. Fernández-Díaz, T. Hansen, H. Gotou, T. Yagi, Y. Ueda, V. I. Anisimov, M. Gruninger, D. I. Khomskii, and M. Braden, Phys. Rev. Lett. **101**, 167204 (2008).
[10] S. V. Streltsov, M. A. Korotin, V. I. Anisimov, and D. I. Khomskii, Phys. Rev. B **78**, 054425 (2008).
[11] S. Mathi Jaya, R. Jagadish, R. S. Rao, and R. Asokamani, Mod. Phys. Lett. B **6**, 103 (1992).
[12] V. I. Anisimov, I. V. Solovyev, M. A. Korotin, M. T. Czyzyk, and G. A. Sawatzky, Phys. Rev. B **48**, 16929 (1993).
[13] M. T. Czyzyk and G. A. Sawatzky, Phys. Rev. B **49**, 14211 (1994).
[14] K. Koepernik and H. Eschrig, Phys. Rev. B **59**, 1743 (1999).
[15] K. Schwarz and P. Mohn, J. Phys. F **14**, L129 (1984).
[16] R. Arita and K. Held, Phys. Rev. B **72**, 201102(R) (2005).
[17] K.-W. Lee, J. Kunes, and W. E. Pickett, Phys. Rev. B **70**, 045104 (2004); K.-W. Lee, J. Kunes, P. Novak, and W. E. Pickett, Phys. Rev. Lett. **94**, 026403 (2005).
[18] M. S. Laad, L. Craco, and E. Müller-Hartmann, Phys. Rev. B **73**, 045109 (2006).
[19] Z. P. Yin, S. Lebègue, M. J. Han, B. P. Neal, S. Y. Savrasov, and W. E. Pickett, Phys. Rev. Lett. **101**, 047001 (2008).
[20] T. Jeong, A. Kyker, and W. E. Pickett, Phys. Rev. B **73**, 115106 (2006).